Submitted to and Accepted by
Applied Physics Letters

Ion acceleration and cooling in gasless self-sputtering

David Horwat[1,2] and André Anders[2a]

[1] Institut Jean Lamour, Département CP2S, UMR 7198 CNRS-Nancy-Université-UPV-Metz, Ecole des Mines de Nancy, Parc de Saurupt, CS14234, 54042 Nancy, France
[2] Lawrence Berkeley National Laboratory, University of California, 1 Cyclotron Road, Berkeley, California 94720, USA

October 31, 2010

ACKNOWLEDGMENT
D.H. acknowledges support by the France-Berkeley Fund under project No. 2009065. Discussions with J. Pelletier and J.-P. Bauer are gratefully acknowledged. This work was supported in part by Berkeley Lab's LDRD program, and in part by the Assistant Secretary for Energy Efficiency and Renewable Energy of the U.S. Department of Energy under Contract No. DE-AC02-05CH11231.

[a] electronic mail, aanders@lbl.gov

Ion acceleration and cooling in gasless self-sputtering

David Horwat[1,2] and André Anders[2b]

[1] Institut Jean Lamour, Département CP2S, UMR 7198 CNRS-Nancy-Université-UPV-Metz, Ecole des Mines de Nancy, Parc de Saurupt, CS14234, 54042 Nancy, France
[2] Lawrence Berkeley National Laboratory, University of California, 1 Cyclotron Road, Berkeley, California 94720, USA

Abstract
Copper plasma with hyperthermal directed velocity (8.8 eV) but very low temperature (0.6 eV) has been obtained using self-sputtering far above the runaway threshold. Ion energy distribution functions (IEDFs) were simultaneously measured at 34 locations. The IEDFs show the tail of the Thompson distribution near the magnetron target. They transform to shifted Maxwellians with the ions being accelerated and cooled. We deduce the existence of a highly asymmetric, pressure-driven potential hump which acts as a controlling "watershed" between the ion return flux and the expanding plasma.

High power impulse magnetron sputtering (HIPIMS) has emerged as an innovation to physical vapor deposition. It combines traditional magnetron sputtering with pulsed power technology resulting in significant ionization of sputtered atoms. This leads to film growth with self-ion assistance, an elegant way to accomplish film densification, improvement of adhesion, and where applicable, control of texture, hardness, elastic modulus, refractive index, and other film properties, and thus has tremendous potential to numerous applications.[1]

The HIPIMS plasma is often dominated by ions of the target material, and hence self-sputtering is an important component of HIPIMS. We speak of sustained self-sputtering (SSS) when sputtering by ions of the target material is sufficient such that the sputtered atoms can be the process "gas".

SSS requires that the self-sputtering parameter $\Pi \equiv \alpha\beta\gamma_{SS}$ equals unity, where α is the probability for a sputtered atom to become ionized, β is the probability that the newly formed ion returns to the target surface, and $\gamma_{SS}(E_i)$ is the self-sputtering yield. The condition $\Pi > 1$ implies self-sputtering runaway, which leads to a very significant increase ("jump") in discharge current as soon as this condition is reached[2]. After a phase of runaway, the system can reach steady-state, $\Pi = 1$, at a very high level of discharge current.

A large fraction (likely > 50%) of newly formed ions needs to return to the target in order to sustain the discharge, yet a very large ion current to a substrate was also observed.[3] This suggests the existence of a potential maximum in the dense plasma ionization zone: ions produced on the target side of the potential maximum have a high likelihood to return to the target, while ions on the substrate side are likely to escape from the magnetron. While most of the anode-cathode potential drop occurs in a thin sheath adjacent to the target ($\leq$ 1 mm), an electric field also exists in the magnetic pre-sheath, which accelerates ions to the sheath edge.[4] However, not much is known about the remaining potential distribution for magnetron plasmas, and in particular for HIPIMS.

[b] electronic mail, aanders@lbl.gov

Brenning and coworkers[5] developed a model of the bulk plasma region of DC and HIPIMS discharges where the potential distribution can be deduced from the electron current density whose surface integral over the discharge cross section must be approximately equal to the discharge current. The generalized Ohm's law can be split in one part describing the electron current density driven by the local electron pressure gradient, $j_e^{\nabla p_e}$,and another part describing the current driven by the local electric field, j_e^E . Lundin *et al.*[6] proposed that the modified two-stream instability (MTSI) is responsible for anomalous current transport, which is driven by the relative drift of electrons and ions, $\mathbf{u_{rel}} = \mathbf{u_i} - \mathbf{u_e}$, in the presence of a magnetic field component perpendicular to $\mathbf{u_{rel}}$. The azimuthal electron current of the magnetron[7] provides the right conditions for the MTSI, leading to perturbations and growing oscillations in the lower hybrid frequency range.[6]

Under the high plasma density conditions of HIPIMS, the condition $j_e^{\nabla p_e} > j_e^E$ can be fulfilled, which enables the existence of the suspected potential hump in the ionization zone. Such potential hump must be very asymmetric since the potential gradient towards the target is extremely steep, while only a few volts over a relatively large distance are needed to remove ions from the ionization zone and accelerate them towards the substrate. DC magnetron discharges do not have a strong electron pressure gradient, and, consistently, no potential hump has been found.[4]

The potential distribution close to a target is very difficult to measure in a direct manner. Therefore, we deduce the potential distribution by measuring a field of ion energy distribution functions (IEDFs). We resort to SSS in the "gasless" HIPIMS mode because scattering of ions by the background gas could destroy the information we seek. Gasless HIPIMS has been demonstrated utilizing a short (20 μs) vacuum arc pulse plasma to trigger the onset of SSS.[8] HIPIMS allows us to go far above the self-sputtering runaway threshold in a very controlled manner.[3]

A set of 36 probes were mounted at four different distances from the center of the target and under angles from 0° to 80° in steps of 10°. The probes are used as Langmuir probes in ion saturation mode and as time-of-flight detectors. The IEDFs were derived from measurements of the velocity distribution functions using a time-of-flight principle previously demonstrated for flowing vacuum arc plasmas.[9] Rapid termination of plasma production leads to a more gradual decay of plasma density at a defined distance from the plasma generator. The decay curve contains information on the ion velocity distribution function using the Laplace transformation[9]

$$f(v) = -c\frac{dI_i(t+t_1)}{dt}, \tag{1}$$

provided the termination was sufficiently rapid, satisfying

$$\left|\frac{1}{I_{dis}}\frac{dI_{dis}}{dt}\right|^{-1} << \left|\frac{1}{I_i}\frac{dI_i}{dt}\right|^{-1}, \tag{2}$$

where I_{dis} is the discharge current, I_i is the ion current at the collecting probe, t_1 is the time of discharge termination, and c is a constant. In contrast to work with conventional energy analyzers, no detailed knowledge of the plasma potential is needed. One has only to make sure that the probe – here used as a time of flight detector – is sufficiently negative with respect to the plasma potential to ensure ion saturation.

The gasless HIPIMS configuration was setup with a planar, nominally balanced magnetron with a 2" (5 cm) diameter target made from oxygen-free high-conductivity (OFHC) copper. The magnetic induction at the center of the target surface was 65 mT; the visible circular racetrack had a diameter of 26 mm. The discharge power was supplied by a SPIK2000A pulse unit (Melec) charged by a Pinnacle supply (Advanced Energy). The potential applied to the target was -1000 V with a pulse duration of 275 μs and a pulse repetition rate of 10 pulses per second. The magnetron discharge was initiated by a short (20 μs) copper vacuum arc of 200 A, with the copper plasma flooding the target surface. The process was conducted at 1 x 10^{-4} Pa, the base pressure of the cryogenically pumped 200 liter chamber.

A 40-channel oscilloscope was used to simultaneously record all relevant information (NI PXI-1045 chassis with five PXI-5105 8-channel digitizer cards, sampling rate 60 MS/second per channel with 12 bit resolution, operated under custom NI LabVIEW software). The data included arc current, magnetron current and voltage, and the currents of the 36 time-of-flight probes. Unfortunately, the probes at 22 cm distance and 40°, and at 30 cm and 30°, developed a short at the feedthrough, thus their data were discarded. The discharge current and voltage were monitored using a broad band current transformer (Pearson) and voltage divider (Tektronix). The probes were mounted on a common holding plate positioned parallel to the target axis and 15 mm below the axis of symmetry to avoid possible shadowing of downstream probes by neighboring upstream probes. Each probe was a disk of 6 mm diameter and 0.5 mm thickness; it was raised 1 mm above the mounting plate such that the probe itself was a shield that prevented shorting by condensing copper. Each probe was individually biased up to −100 V with respect to ground (= anode potential of arc source and magnetron). A schematic of the same probe set for an experiment in gas can be found in another paper.[10]

Figure 1 shows the signals of the probes with the time zero assigned to the end of the discharge pulse. The discharge had reached a steady-state as evident by the constant discharge current (not shown here). The local plasma density in the steady-state can be determined from the ion saturation current I_{sat} to the probe's collecting area A_{probe} using $n_i = I_{sat} \big/ \left(A_{probe} e\, u_{i,probe} \right)$, where we used the ion thermal velocity $u_{i,probe}$ with the justification that most of the probe area is aligned parallel to the flow from the target. With those assumptions we obtain a local ion density of 5×10^{18} m^{-3} for the probe at 60 mm, 0°, and falling as $n_{\text{i,steady-state}}\left(z, 0°\right) \propto z^{-1.65}$. The exponent is smaller than -2, which is consistent with the observation that the magnetron is not a point source for spherical expansion but rather "throws" sputtered material in a preferred direction, the target normal. Extrapolation of the $z^{-1.65}$ fit back to $z \approx 30\,\mathrm{mm}$ gives 1.4 x 10^{19} m^{-3}, which is indicative of the very high densities above the runaway threshold. The densities at the other probes are proportional to their currents as shown in Fig. 1.

The decay curves of Fig. 1 were used to derive the ion velocity distribution functions which in turn were converted to the IEDFs shown in Fig. 2. The initial ion distributions have their origin in the energy distribution of sputtered atoms. Following the Sigmund-Thompson theory[11-12] they can be approximated by

$$f_{\text{Thompson}}\left(E\right) \propto \frac{E}{\left(E + E_{SB}\right)^3} \tag{3}$$

which has been included in Fig. 2 using the surface binding energy for copper, $E_{SB}\left(\mathrm{Cu}\right) = 3.49\ \mathrm{eV}$ [13]. The distribution (3) has a peak at $E_{SB}/2$ and falls with E^{-2}. Data taken

at 6 cm from the target center show the characteristic E^{-2} tail but the peak region, with much slower ions, had already thermalized to a shifted Maxwellian distribution,

$$f_{\text{S-Maxwell}}(E) \propto E \exp\left(-\frac{\sqrt{E}-\sqrt{E-E_{dir}}}{T_i}\right), \tag{4}$$

which is well known for streaming vacuum arc plasmas[14]. Fitting of (4) to the data gives values for the ion temperature and directed energy, T_i and E_{dir}, from the width and shift of the distribution, respectively. Since data are available for the various locations we can derive the evolution of the IEDF as ions move away from the ionization zone. We see that the ions acquire an average kinetic energy of about 8.8 eV, while they cool down to a temperature of only 0.6 eV. To understand those values we need to consider pressure gradients and collisions.

The sputtered atoms will collide with neighboring atoms. The thermalization length is about 5 cm for copper atoms moving in 1 Pa of argon.[15] In the self-sputtering regime investigated here, the "gas" moves away from the target, and thermalization occurs in a frame of reference moving with the "sputter wind".[16] The dense HIPIMPS plasma occupies a near-target zone that sputtered atoms have to pass before they could arrive at the substrate, and in doing so, there is an appreciable probability of ionization. Given the arch formed by the magnetic field lines, the densest plasma zone is about $z_{\text{dense}} = r_{\text{race}} - s_{\text{target}}$ above the racetrack, where r_{race} is the radius of the racetrack (13 mm for our magnetron), and s_{target} is the target thickness (5 mm). We see that even the closest probes at 60 mm are far from the ionization zone.

When an atom becomes ionized by electron impact, its kinetic energy remains practically unchanged due to the small mass of the electron. Thus it is expected that the IEDFs initially exhibit the features of a Thompson distribution. Via ion-ion collisions, the distribution changes towards the equilibrium distribution, which is a Maxwellian. The shifts measured in the laboratory frame of reference are due to the initial directed flux from the sputtering process and forces of pressure gradients and electric fields.

The frequency of ion-ion momentum exchange collisions can be calculated using Spitzer's formula

$$\nu_{ii}(z) \approx C \frac{n_i(z)}{m_i^{1/2}\left(k T_i(z)\right)^{3/2}}, \tag{5}$$

where $C = e^4 \ln\Lambda / 12\pi^{3/2}\varepsilon_0^2 \approx 1.3\times10^{-54}\,(\text{AsVm})^2$ and we assumed single charge state; k is the Boltzmann constant, ε_0 is the permittivity of free space, and $\ln\Lambda \approx 10$ is the Coulomb logarithm. We find that the average time between collisions $\tau_{ii} = \nu_{ii}^{-1}$ is in the sub-microsecond range in the dense plasma zone, increasing to tens of microseconds for the expanding plasma at z > 10 cm. Therefore, slow ions are well thermalized by the time they arrive at the first set of probes (6 cm) while ions in the energetic tail of the distribution travel much further before being thermalized. We can detect remnants of the Thompson distribution tail in the IEDFs at 30 cm. The main finding, however, is that the *IEDFs exhibit a systematic shift to higher energies as the ions move away from the target*.

The concept of a pressure-driven establishment of a potential hump, which controls the current balance for HIPIMS discharges, requires that the hump adjusts appropriately if the power is changed. Experiments with different HIPIMS voltage settings confirmed that the ion energy shift is approximately proportional to the discharge voltage above the runaway threshold.

Without further elaboration (for space reasons) we report that the hump increases by about 1 V for every 100 V above the self-sputtering runaway threshold, which is at about 530 V.

We conclude that gasless self-sputtering, and specifically when operated in HIPIMS mode far above the runaway threshold, delivers flowing plasma with hyperthermal ion velocity (~ 9 eV) and very low ion temperature (0.6 eV). The deduced potential hump appears to be a critical mechanism for the regulation of current balances and the concept may also be applicable to situations other than those investigated here.

D.H. acknowledges support by the France-Berkeley Fund under project No. 2009065. Discussions with J. Pelletier and J.-P. Bauer are gratefully acknowledged. This work was supported in part by Berkeley Lab's LDRD program, and in part by the Assistant Secretary for Energy Efficiency and Renewable Energy of the U.S. Department of Energy under Contract No. DE-AC02-05CH11231.

References

[1] K. Sarakinos, J. Alami, and S. Konstantinidis, Surf. Coat. Technol. **204,** 1661 (2010).
[2] A. Anders, J. Andersson, and A. Ehiasarian, J. Appl. Phys. **102,** 113303 (2007).
[3] J. Andersson and A. Anders, Phys. Rev. Lett. **102,** 045003 (2009).
[4] J. W. Bradley, S. Thompson, and Y. A. Gonzalvo, Plasma Sources Sci. Technol. **10,** 490 (2001).
[5] N. Brenning, I. Axnas, M. A. Raadu, D. Lundin, and U. Helmersson, Plasma Sources Sci. Technol. **17,** 045009 (2008).
[6] D. Lundin, U. Helmersson, S. Kirkpatrick, S. Rohde, and N. Brenning, Plasma Sources Sci. Technol. **17,** 025007 (2008).
[7] J. Bohlmark, U. Helmersson, M. VanZeeland, I. Axnäs, J. Alami, and N. Brenning, Plasma Sources Sci. Technol. **13,** 654 (2004).
[8] J. Andersson and A. Anders, Appl. Phys. Lett. **92,** 221503 (2008).
[9] E. Byon and A. Anders, J. Appl. Phys. **93,** 1899 (2003).
[10] D. Horwat and A. Anders, J. Appl. Phys.**,** submitted.
[11] P. Sigmund, Phys. Rev. **184,** 383 (1969).
[12] M. W. Thompson, Phil. Mag. **18,** 377 (1968).
[13] Y. Yamamura and H. Tawara, Atomic Data and Nuclear Data Tables **62,** 149 (1996).
[14] J. Rosén, A. Anders, S. Mráz, A. Atiser, and J. M. Schneider, J. Appl. Phys. **99,** 123303 (2006).
[15] W. D. Westwood, J. Vac. Sci. Technol. **15,** 1 (1978).
[16] W. D. Hoffman, J. Vac. Sci. Technol. A **3,** 561 (1985).

Figure Captions

Fig. 1 Ion saturation currents simultaneously measured by 34 probes (Cu target, -1000 V applied voltage, 275 μs pulse duration, 10 pulses per second). Note that the time scale was kept the same but the amplitude scale was adjusted for best display.

Fig. 2 Ion energy distribution functions in the steady-state phase of gasless sputtering of copper, as derived from the ion velocity distribution functions at the positions indicated. The Thompson distribution of sputtered atoms and a best fit of shifted Maxwellian distribution functions are added.

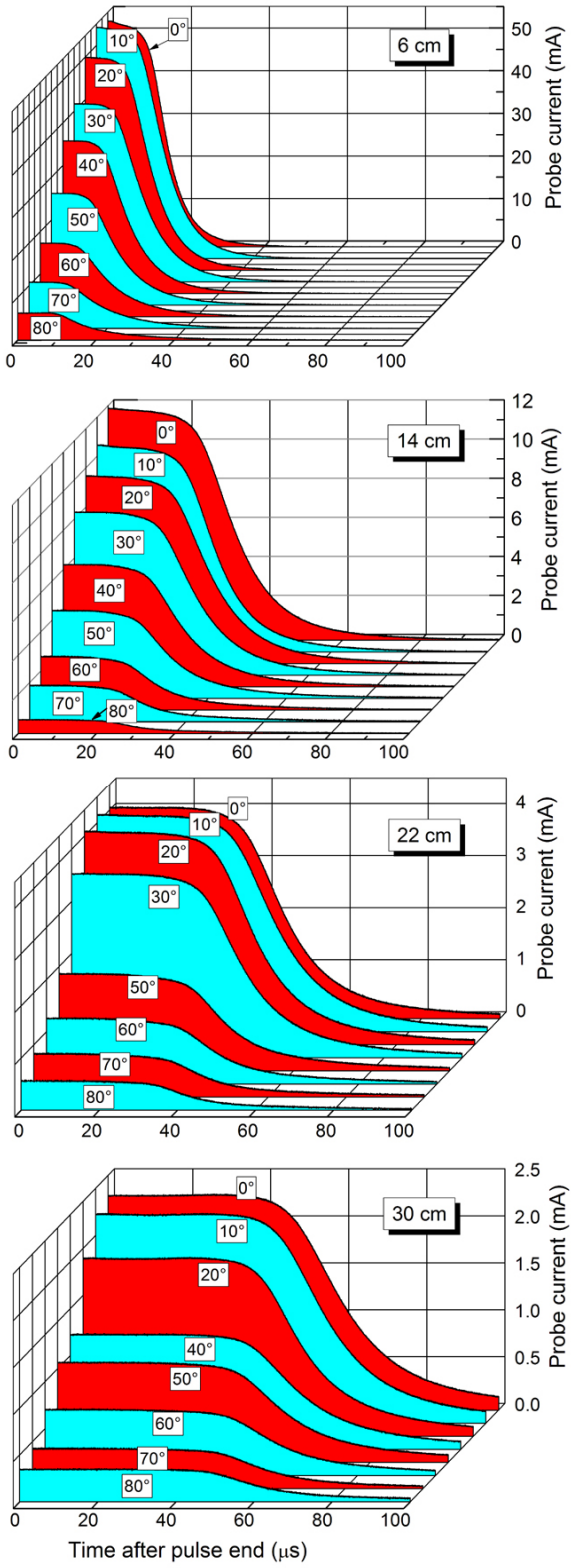
6 cm
14 cm
22 cm
30 cm
0°
10°
20°
30°
40°
50°
60°
70°
80°
Probe current (mA)
Time after pulse end (μs)

Fig. 1

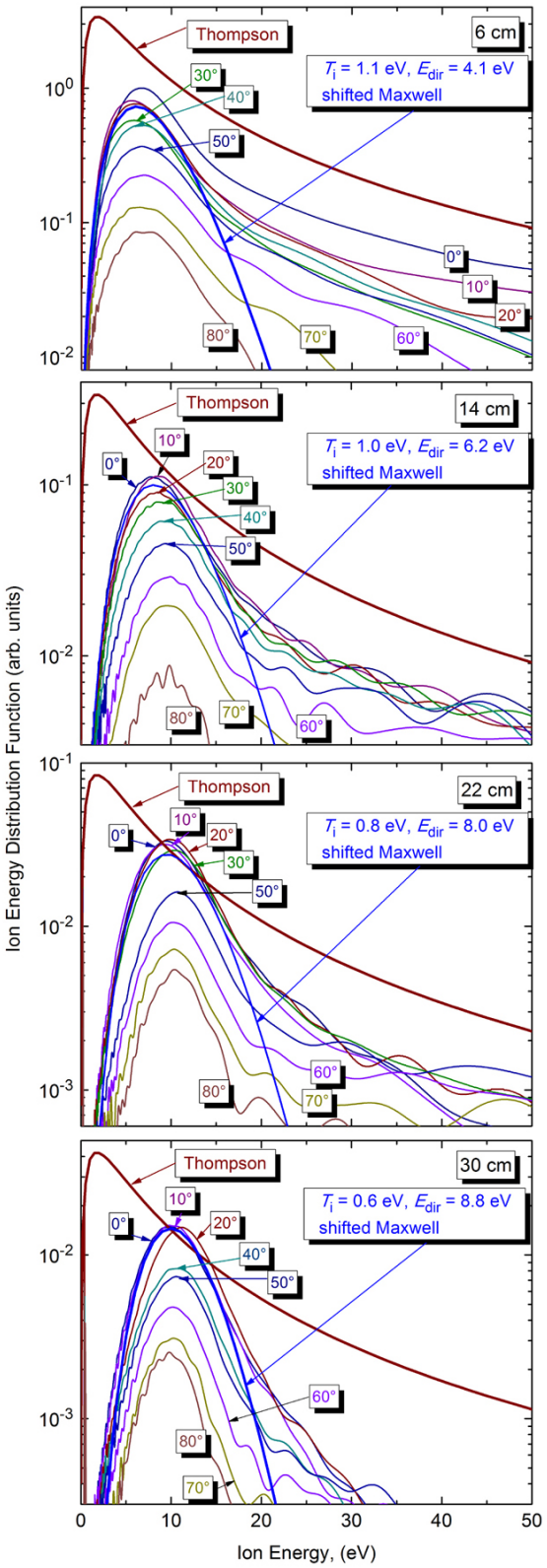
Thompson
6 cm
T_i = 1.1 eV, E_{dir} = 4.1 eV
shifted Maxwell
14 cm
T_i = 1.0 eV, E_{dir} = 6.2 eV
22 cm
T_i = 0.8 eV, E_{dir} = 8.0 eV
30 cm
T_i = 0.6 eV, E_{dir} = 8.8 eV
Ion Energy Distribution Function (arb. units)
Ion Energy, (eV)

Fig. 2